Published in final edited form as:
*Biomaterials*. 2014 March ; 35(9): 2752–2759. doi:10.1016/j.biomaterials.2013.12.039.

# The effect of mesenchymal stem cell sheets on structural allograft healing of critical-sized femoral defects in mice

**Teng Long**[1,2,†], **Zhenan Zhu**[1,†], **Hani A. Awad**[2], **Edward M. Schwarz**[2], **Matthew J. Hilton**[2], and **Yufeng Dong**[2,*]

[1]Department of Orthopaedics, Ninth People's Hospital, Shanghai Jiaotong University School of Medicine, 639 Zhizaoju Road, Shanghai, 200011 China

[2]The Center for Musculoskeletal Research, Department of Orthopaedics and Rehabilitation, University of Rochester Medical Center, 601 Elmwood Avenue, Box 665, Rochester, NY 14642, USA

## Abstract

Structural bone allografts are widely used in the clinic to treat critical sized bone defects, despite lacking the osteoinductive characteristics of live autografts. To address this, we generated revitalized structural allografts wrapped with mesenchymal stem/progenitor cell (MSC) sheets, which were produced by expanding primary syngenic bone marrow derived cells on temperature-responsive plates, as a tissue engineered periosteum. *In vitro* assays demonstrated maintenance of the MSC phenotype in the sheets, suggesting that short-term culturing of MSC sheets is not detrimental. To test their efficacy *in vivo*, allografts wrapped with MSC sheets were transplanted into 4-mm murine femoral defects and compared to allografts with direct seeding of MSCs and allografts without cells. Evaluations consisted of x-ray plain radiography, 3D microCT, histology, and biomechanical testing at 4- and 6-weeks post-surgery. Our findings demonstrate that MSC sheets induce prolonged cartilage formation at the graft-host junction and enhanced bone callus formation, as well as graft-host osteointegration. Moreover, a large periosteal callus was observed spanning the allografts with MSC sheets, which partially mimics live autograft healing. Finally, biomechanical testing showed a significant increase in the structural and functional properties of MSC sheet grafted femurs. Taken together, MSC sheets exhibit enhanced osteogenicity during critical sized bone defect repair, demonstrating the feasibility of this tissue engineering solution for massive allograft healing.

## Introduction

Massive bone grafting is commonly used in both military and civilian orthopaedic reconstruction surgeries to repair critical sized defects due to trauma or tumor resection. Both experimental and clinical studies have demonstrated that live autologous grafts are superior to processed or devitalized allografts when analyzing bone incorporation, repair, and remodeling [1, 2]. However, due to the limited availability of autologous bone grafts, and problems with chronic pain at the donor site [3, 4], processed allografts remain an attractive substitute for bone grafting. It has long been recognized that there are several fundamental differences between a live autograft and a processed allograft including: i)

*Address correspondence to: Yufeng Dong, MD&PhD, Center for Musculoskeletal Research, Department of Orthopaedics and Rehabilitation, University of Rochester School of Medicine, 601 Elmwood Avenue, Box 665, Rochester, NY 14642, Phone: (585) 273-2235, Fax: (585) 275-1121, Yufeng_Dong@urmc.rochester.edu.
†Both authors contributed equally to this work

**Author contributions:** Y.D., M.J.H., E.M.S obtained the funding; Y.D., M.J.H., H.A., E.M.S, and Z.Z. designed all experiments; T.L and Y.D. performed in vitro and in vivo studies.

autografts contain living cells that can produce new bone [5, 6]; ii) autografts contain growth factors and osteogenic substances; and iii) the host can effectively remodel the autograft but does not resorb the processed allograft [7, 8]. Clinically, more than 500,00 Americans require bone allografts annually, although due to the lack of appropriate osteogenesis, angiogenesis and remodeling of structural allografts, the 10-year post-implantation failure rate is 60% [9]. Thus, the major challenge to the field of bone grafting is to identify the central factors, cells, and/or environmental cues that govern normal autograft healing and to devise a method to achieve the same healing results when utilizing processed allografts.

There are at least three experimental approaches that have been devised to enhance the osteogenic response of structural allografts. The first strategy involves the delivery of recombinant protein growth factors locally with the allograft (i.e. bone morphogenetic proteins; BMPs) [10, 11] or systemically (i.e. parathyroid hormone; PTH) [12] via treatment of the host. Despite the applicability of these approaches, sustaining local growth factor delivery and regulating the influence of growth factors on non-targeted cell populations remains a substantial barrier to tissue engineering and has presented significant safety concerns and complications in some clinical settings [13–15]. While treatments with osteogenic factors show promise, they also rely heavily on the host to provide the appropriate number of cells with which to mount an adequate osteogenic healing response. These host requirements exist regardless of the treatment regimen, dose, or delivery method. The second strategy utilizes viral and/or non-viral targeted osteogenic or angiogenic gene delivery approaches [16, 17]. While a few of the gene transfer methods for critical defect healing have reached orthopaedic pre-clinical trials, there remain significant regulatory, efficacy, and safety concerns with the use of viral agents or genetically altered cells for implantation into patients. The third and possibly the most exciting strategy to promote or enhance devitalized allograft incorporation and critical sized bone defect healing involves the use of the patient's own mesenchymal stem/progenitor cells (MSCs). This approach, currently in experimental phases, entails the isolation of bone marrow derived MSCs from a patient and seeding the cells on a graft or scaffold prior to transplantation. While this approach has demonstrated some success with marrow-derived MSCs, experimental strategies have primarily been focused on ensuring the appropriate engraftment of MSCs into host bone when using scaffold or allograft carriers [18–21].

The most well studied and clonogenic MSC populations commonly express a number of cell surface markers including CD105, CD90, CD106, CD146, CD29, and CD166, and lack the expression of hematopoietic lineage markers, including CD34, CD11b and CD45 [22, 23]. Cell surface markers such as SSEA4, CD105, Sca1, and Stro-1 have been successfully used to enrich MSC populations [24–26]. MSC populations, however, tend to lose their multipotency and capacity to proliferate with increasing passages in culture, suggesting senescence [27]. Growth factors such as FGF2 and FGF4 have been utilized to promote the expansion of MSC populations [28, 29], while some of the well known stem cell transcriptional regulators (*SOX2*, *OCT4*, *NANOG*) have also been used to promote the maintenance and multipotency of MSCs in culture [30, 31]. In this study, we utilized a set of these stromal cell markers to evaluate changes in cellular behavior during cell isolation and generation of MSC sheets.

Cell sheet technology has been applied in tissue engineering for several years to regenerate damaged soft tissues, including corneal epithelia [32], periodontal ligament cells [33], bladder epithelia [34], kidney glomeruli [35], oesophageal epithelia [36], myocardial cells [37] and hepatocytes [38]. Cell sheet technology consists primarily of a "thermo-responsive culture dish" which enables reversible cell adhesion to and detachment from the dish surface by controlling the hydrophobicity of the surface [39]. This allows for a non-invasive harvest of high-viability cells in an intact monolayer that includes any deposited extracellular matrix

(ECM). The ECM provides the necessary structural and adhesive properties for maintaining cell sheet integrity and resisting deforming forces during transplantation. Through implementation of this technology, MSC sheets can be easily generated and transplanted to the site of large bone defects, acting as a tissue-engineered periosteum surrounding the implanted graft. We expect that the utilization of MSC sheets will enhance allograft incorporation into the host bone without necessitating the use of a biodegradable scaffold.

In this study, we first utilized temperature-responsive culture dishes in the generation of human MSC sheets *ex vivo*. Second, we used these cells to test the hypothesis that allografts used in conjunction with MSC sheets possess superior osteogenic properties and enhanced bone defect healing during skeletal repair in a preclinical mouse model of critical sized femoral allograft.

## Materials and Methods

### Study design

Experiments were designed to include six male mice samples per group at different time point. Host mice carrying allografts were randomly and equally assigned to either control, MSC-seeding or MSC-sheet groups. The sample size for Micro-CT and biomechanical testing was determined by power analysis based on our pilot experiment data.

### Mouse strains

C57BL/6J mice were purchased from Jackson Laboratory. Allogeneic bone grafts were obtained from mice of the 129/J strain for implantation into C57BL/6J mice. The University of Rochester Committee of Animal Resources approved all animal surgery procedures.

### Bone marrow MSC isolation

Bone marrow derived MSCs were isolated from 6-week old C57BL/6J mice using a modified version of a previously described protocol [40]. In brief, mice were sacrificed by $CO_2$ asphyxiation followed by cervical dislocation. Femurs and tibiae were dissected from the surrounding tissues. The epiphyseal growth plates were removed and the bone marrow was collected by flushing with αMEM culture medium containing 100 U/ml Penicillin, 100μg/ml streptomycin and 10% FCS (Hyclone) with a 25-gauge needle. Single cell suspensions were prepared by gently mixing the cells with a pipette followed by filtration through a 70-μm strainer. 2–5 × $10^7$ total bone marrow cells were obtained using 5–10 mice. The EasySep Mouse Mesenchymal Progenitor Enrichment Kit (Stem Cell Technologies) was used as a negative selection strategy to remove unwanted cells of the hematopoietic and endothelial lineages (CD45, TER119 antibodies linked to magnetic beads) according to manufacturer's instructions. Remaining viable cells were counted using trypan blue staining and re-seeded at 500 cells/$cm^2$ and grown in Mesenchymal Stem Cell Growth Medium for expansion. Media were replaced 3 days and refreshed 6 days post adherence. At day 7, cells were harvested for colony forming units-fibroblast (CFU-F) assay and a second in vitro expansion. To monitor the colony formation, some of the colonies were fixed using 4% PFA and stained with 0.2% crystal violet solution for 1 hour before they were washed with water and images were captured. Colonies consisting of at least 50 cells were counted as CFU-Fs.

### Generation of MSC sheets

When cells reached 80% confluence during the second expansion, some of the cells were then harvested for flow cytometry analysis and the rest of the MSCs were re-seeded at 3 different densities (200, 100, 50 cells/$mm^2$) on thermo-responsive 6-well culture plates with UpCell surface (Thermo Scientific, Cat. 174901) to generate cell sheets. Once the cells

reach 100% confluence (monolayer cell sheet), cell sheets were harvested for flow cytometry, RNA isolation, and in vivo implantation. MSCs at 80% confluence were used for RNA isolation and flow cytometry as a control.

### Cell viability assay

After 24 hours of culture, newly formed MSC sheets were trypsinized using 0.25% trypsin-EDTA (Invitrogen) and then stained with 0.4% trypan blue solution. Cell viability was estimated by cell counting via hemocytometer in which non-viable cells appear blue, viable cells are unstained.

### Flow cytometry analysis

Following the second expansion, cells were trypsinized and stained with 0.2ug of CD105 antibody conjugated to FITC, 0.2ug of CD29 antibody conjugated to PE, and 0.2ug of Sca-1 antibody conjugated to APC (ebioscience). After washing in FACS buffer, the cells were analyzed on an LSR-II (Beckton Dickson) and the data were further analyzed using FlowJo software (Tree Star). MSCs at 80% confluence and cell sheets were also collected for Flow cytometry analysis using the CD105 antibody.

### Real-time PCR analysis

Total RNA was isolated from MSCs using RNeasy Mini Kit from Qiagen Inc. One microgram of RNA was subjected to reverse transcription using the iScript cDNA synthesis Kit (Bio-Rad). The obtained cDNA was then amplified via real-time PCR using an ABI 7500 Real-time PCR System (Applied Biosystems) and SYBR® Green Real time PCR Supermix (Bio-Rad). The primers used for real-time PCR are listed in Table 1, and β-actin was used as the housekeeping gene. Quantification of the relative expression levels of these target genes was achieved by normalizing to β-actin using the ΔΔCt method.

### Devitalization of bone allografts

Eight week-old male 129/J mice were used for donation of devitalized allografts. Briefly, mice were euthanized and a 4mm mid-diaphyseal segment was removed from each femur by osteotomy using a rotary Dremel with custom circular diamond blades. Allograft segments were flushed of the bone marrow using 25-guage needles, the periosteal tissues were manually stripped, and the bone grafts were washed repeatedly in 70% ethanol for at least 4 hours. The allografts were then stored in 100% ethanol at −80°C for at least 7 days to complete the devitalization process.

### Wrapping of MSC sheets on allografts

Following MSC sheet formation, cell sheets were wrapped onto devitalized allografts. Briefly, the cultured MSC sheets were covered by a cell transfer membrane (Thermo Scientific, Cat.1749016) and kept at 25°C for 10 min. After the cell layer adhered to the membrane, it was detached carefully from the thermo-responsive culture plate. The cell sheet and membrane were then placed in a new larger dish with the cell layer facing up, the devitalized room temperature allografts were placed on the top of cell sheets and wrapped by one layer of cell sheet and incubated for an additional 30 minutes at 37°C in fresh media to release the membrane. After carefully removing the membrane from the cell sheet, the MSC sheet wrapped allografts (MSC-sheet) were kept at 37°C for allograft transplantation surgery. Additionally MSCs were seeded directly onto devitalized allografts (MSC-seeded) via cell culture methods as described previously [41]. Briefly, the grafts were placed in 48 well culture plates containing standard media for 30 min prior to the initial seeding of $5\times10^5$ MSCs. MSCs were allowed to incubate for an additional 30 minutes at 37°C on the grafts. The grafts were rotated 180° and another $5\times10^5$ MSCs were seeded onto the other side of

the graft in an attempt to generate an even distribution of MSCs across the graft. The MSCs directly seeded onto allografts were incubated at 37°C for about 1 hour to allow the cells to attach and integrate into the graft prior to transplantation.

### Surgical reconstruction of the mouse femoral defects

8-week-old C57BL/6J mice were anesthetized via intraperitoneal injection with a combination of ketamine (60mg/kg body weight) and xylazine (4mg/kg body weight). A 7–8mm long incision was made, and the midshaft femur was exposed using blunt dissection of muscles. A 4-mm mid-diaphyseal segment was removed from the femur by osteotomizing the bone using the Dremel tool. A 4-mm cortical bone graft with/without MSCs or MSC sheet was then inserted into the segmental defect and stabilized using a 26-gauge metal pin placed through the intramedullary marrow cavity, as previously described [41]. The incisions were closed using silk sutures. Graft healing was followed radiographically using a Faxitron X-ray system (Faxitron X-ray Corporation, Wheeling, IL). Mice were sacrificed at 2, 4, and 6 weeks post surgery and samples processed for further analysis.

### Micro-CT bone imaging analyses

Some of the reconstructed femurs from weeks 4 and 6 (n=6) were imaged after careful dissection and removal of the intramedullary pin using a microCT system (VivaCT 40, Scanco Medical). Briefly, the femurs were scanned using a protocol that utilizes high-resolution (10.5 microns) x-ray energy settings of 55 kVp and 145 μA. Quantification of bone volume and total volume of callus were performed as previously described using the Scanco analysis software [42].

### Biomechanical testing

Specimens (n=6) from day 42 were harvested and moistened with saline before biomechanical testing. The ends of the femurs were cemented into square aluminum tube holders using PMMA to ensure axial alignment and to maintain a gage length of 7–8 mm, allowing a length of at least 3mm to be potted at each end. Specimens were mounted on an EnduraTec TestBench™ system (200 N.mm torque cell; Bose Corporation) and tested in torsion until failure. The torque data were plotted against the rotational deformation (normalized by the gage length and expressed as rad/mm) to determine the Maximal Torque and torsional rigidity.

### Histological evaluation of grafted femurs

The femoral samples to be used for histology analyses were fixed in neutral buffered formalin and processed in paraffin. Paraffin embedded samples (n=6) from weeks 4 and 6 were sectioned at 5μm. Sections were stained with Alcian Blue/Hematoxylin/Orange-G (AB/H/OG) to determine the contributions of cartilage, bone, and fibrotic tissue during the repair process.

### Statistical analysis

The above experiments were repeated at least three times independently. All data are presented as mean ± SD. Statistical significance among the groups was assessed using one-way ANOVA. The level of significance was $P < 0.05$.

## Results

### MSC isolation and cell sheet culture

Since bone marrow derived MSCs (BMSCs) are readily available and have extensive osteogenic differentiation potential, we utilized these cells for generating periosteum-like

MSC sheets for *in vivo* implantation and the enhancement of allograft incorporation. We first isolated BMSCs from 6-week-old C57BL/6J mice (n=5) using the EasySep Mouse Mesenchymal Progenitor Enrichment Kit. After pre-enrichment through negative selection, the cell clonogenic ability of MSCs was tested by CFU-F assays. A yield of 100–150 CFU-F colonies was obtained, following 7 days in culture with an initial seeding density at 500 cells/$cm^2$. Fig. 1A shows a representative CFU-F that contains fibroblast-like mesenchymal progenitor cells and suggests that our isolation technique is suitable for preparation of MSCs with self-renewal ability. To obtain sufficient numbers of MSCs for further experiments, all colonies were collected and re-cultured for an additional 7 days *in vitro* before harvesting for flow cytometry analysis and cell sheet preparation. Flow cytometry analyses demonstrated that cells obtained from three separate preparations ranged from 63.6% to 91.6% positive for stem cell markers CD105 (Fig. 1B), CD29 (Fig. 1C) and Sca1 (Fig. 1D). The average expression of these three MSC cell surface markers from all populations was further shown in Fig. 1E. These data suggest that our MSC preparations are enriched with cells expressing common MSC cell surface markers, and therefore they were utilized for subsequent *in vivo* tissue regeneration experiments.

For culturing MSC sheets, MSCs were re-seeded on thermo-responsive 6-well (960$mm^2$/well) culture plates at 3 different cell densities. After 24 hours of culture, MSCs successfully formed monolayer sheets with cell seeding at 200 cells/$mm^2$ (Fig. 2B), and this newly formed MSC sheet was easily detached from the dish for transfer after incubation at 25 °C for 10 min (Fig. 2C). To assess cell density and viability after cell sheet culture, a newly formed monolayer MSC sheet was trypsinized and stained with trypan blue. Approximately 1.0 million cells were counted in a sheet (1000 cells/$mm^2$) and less than 5% of these cells were stained by trypan blue, suggesting short-term cell sheet culture did not significantly change MSC viability *in vitro*. We further observed that 3-days of culture were required to form cell sheets at 50 cells/$mm^2$ and 5-days for 10 cells/$mm^2$ (data not shown). These data suggest that at least 200,000 cells are required at initial seeding to form a 960$mm^2$ cell sheet in 24-hours. This size is compatible with generating around 32 tissue-engineered periostea for the 4-mm allograft segment (surface area is around 30$mm^2$) used in our skeletal repair mouse model (Fig. 2D).

To determine whether this short-term (24-hours) cell sheet culture would significantly change the existing MSC phenotype, we further performed real-time qPCR for *Sox2*, *Oct4*, *Nanog*, and *CyclinD1* (MSC markers of stemness and proliferation), as well as, flow cytometry for CD105 in cells before (80% confluent, Fig. 2A) and after cell sheet formation (Fig. 2B). qPCR results showed no significant change in the gene expression for any of the MSC or proliferative markers (Fig. 2E), with only mild changes in the number of CD105 positive MSCs (63% in 80% confluent cultures compared to 53% in cell sheets). These data indicate that short-term culture of MSCs to generate cell sheets does not significantly alter the MSC phenotype.

## MSC sheets increase bone formation and osteointegration of femoral allografts

To test whether this MSC sheets can be used *in vivo* as a pseudo-periosteum to enhance allograft bone defect healing, we transplanted allografts alone (Fig. 3A, D, G, J), allograft with direct-culture seeded MSCs (Fig. 3B, E, H, K), or allografts wrapped with MSC sheets (Fig. 3C, F, I, L) into our mouse femoral bone defect model. 2 weeks after surgery, X-ray results showed no significant difference in bony callus formation around allografts in all 3 groups (Data not shown). At 4 weeks, newly formed bony callus was observed surrounding each end of the allografts for both MSC-seeded groups (Fig. 3B) and MSC-sheet groups (Fig. 3C). However, the callus size was considerably larger in the MSC sheet groups, indicating a more mineralized and robust bone formation response. In contrast, no bony

callus was observed in the allograft alone groups (Fig. 3A). At 6 weeks, a minimal amount of new callus was observed between the allograft and host bone in the allograft alone groups (Fig. 3D). MSC-seeded allografts exhibited large bony callus formation near the allograft and host bone junction, but no significant callus formation was ever observed near the mid-allograft surface (Fig. 3E). In contrast, a large bridging callus was observed surrounding the allograft in MSC-sheet groups and the gap between allograft and host bone had disappeared due to the formation of a bony union (Fig. 3F). AB/H/OG stained sections confirmed that at 4 weeks a cartilaginous soft callus formed at the host/allograft junction in both MSC-seeded (Fig. 3H) and MSC-sheet groups (Fig. 3I). Interestingly, more woven bone surrounded the allograft in MSC-sheet groups as compared to other groups. In contrast, no significant callus formation was observed in the allograft alone group (Fig. 3G). Consistent with X-ray data, at 6 weeks only the MSC-sheet groups exhibited a completely remodeled woven bone callus without cartilage surrounding the allograft (Fig. 3L). By contrast, the callus from allograft alone (Fig. 3J) and MSC-seeded group (Fig. 3K) demonstrated persistent cartilage between the allograft and callus tissues at 6 weeks.

To further confirm our X-ray and histological findings, we performed microCT analysis using samples from 4- and 6-weeks post-surgery. MicroCT analyses demonstrated that the size of the external callus at the host/allograft junction in both MSC-seeded (Fig. 4B, H) and MSC-sheet groups (Fig. 4C, I) were larger and contained more mineralized bone than the allograft alone groups (Fig. 4A, G) at 4 and 6 weeks post-transplantation. Cut-sections of the microCT images for the entire repair region further demonstrated that a bony union was achieved only in the MSC-sheet groups at 6 weeks post-surgery (Fig. 4L), while the gap between allograft and host bone was still visible in both allograft alone (Fig. 4J) and MSC-seeded groups (Fig. 4K). Although we did not see an obvious increase in callus formation specifically at the host/allograft junction in MSC-sheet groups when compared to MSC-seeded groups, we did observe a substantial bony callus extending across nearly the entire surface of the allograft of the MSC-sheet groups (Fig. 4I, L). Finally, the percentage of bone volume (BV) to total tissue volume (TV) of callus was calculated and identified to be significantly higher in the MSC-sheet groups when compared to both culture-seeded MSC groups and allograft alone groups at 4 and 6-weeks post-transplantation (Fig. 4M).

### MSC sheets increase the biomechanical properties of femoral allografts

In order to determine whether the MSC sheet-induced histologic and radiographic increases in bone callus volume translated into improved mechanical properties, we performed torsional testing on the grafted femurs at 6-weeks post surgery. While MSC-seeded groups showed an increase in bone callus formation during skeletal repair, we did not detect a significant increase in the maximum torque as compared to allograft alone groups (Fig. 5A). However, a mild increase in torsional rigidity (Fig. 5B) was observed between the MSC-seeded groups and the allograft alone groups. In contrast to MSC-seeded groups, a significant increase in maximum torque and torsional rigidity was shown in MSC-sheet groups [20.1 N.mm and 543.7 $N.mm^2$/rad, respectively] when compared to MSC-seeded and allograft alone groups (Fig. 5A, B). Collectively, these data demonstrate that the use of MSC-sheets during allograft repair of critical sized bone defects induces *de novo* bone formation across the graft leading to a stronger and more mineralized bone union.

## Discussion

The major complications associated with large structural bone allografts used to reconstruct segmental skeletal defects are fractures and nonunions [43]. This may be largely due to the absence of multipotent MSCs from the periosteum or bone marrow. Removal of the periosteum from bone autografts markedly impairs healing, whereas engraftment of

mesenchymal progenitor cells on bone allografts improves healing and graft incorporation [44]. Although the ability of MSC populations to enhance allograft repair has been recognized, attaining the appropriate delivery and retention of MSCs for skeletal repair therapeutic strategies has proven to be difficult. Cell culture techniques in which MSCs have been directly cultured on allografts have demonstrated some success, however problems remain. Two significant problems are the uneven cell distribution across allografts and the weak adhesion of MSCs seeded on the allograft, which can result in detachment following surgical transplantation. To overcome these problems, biodegradable polymer scaffolds have been used with cells to fabricate three-dimensional tissue-like grafts in addition to, or instead of, allograft approaches. However, strong inflammatory responses are often observed upon biodegradation of the scaffolds. Macrophages and neutrophils with collagenase and elastase activities migrate to the implantation site during the early wound healing response. This host inflammatory response can damage the seeded cells even though the biodegradable scaffolds are non-toxic and mechanically non-invasive, resulting in the failure of the engineered tissues [45]. Therefore, a new method that circumvents the use of biodegradable scaffolds for MSC delivery is required for allograft transplantation.

Since cell sheet technology has been successfully used in the regeneration of other soft tissues (i.e. cornea, heart, esophagus) as we mentioned above, we explored whether MSC sheets could serve as an ideal approach for the local delivery of cells to enhance allograft repair and integration. In this study we utilized a heterogeneous population of MSCs isolated from mouse bone marrow, which contains CD105, CD29, and Sca1 positive cells and is thought to be enriched with bona fide skeletal stem cells. The presence of these markers suggests at least some of the skeletal stem cells are present in our heterogeneous MSC populations. By generating MSC sheets using the protocol and technology described herein, we were able to form cell sheets with sufficient biomechanical strength to avoid breakage during surgery and transplantation. Although, monolayer MSC sheets generated in 6 hours or less by seeding a high density of cells was more susceptible to rupture and deformation during transplantation. This is likely due to the deposition of a lesser ECM during the shortened culture period. Since our flow cytometry data indicated no significant changes in the gene expression for any of the MSC or proliferative markers after 24 hours of MSC sheet culture, we selected this time-point for the generation of our MSC sheets. While the stem cell surface marker CD105 exhibited a mild decrease in expression in cultured MSC sheets, our data suggests that this did not significantly affect the osteogenic ability of cell sheets *in vivo*, although the identification and use of a more pure skeletal stem cell population would likely provide even greater skeletal repair potential. While the exact cell source may be important, the cell sheet itself is also critical for providing normal, undisturbed cell-cell interactions and the development of an ECM that promotes cellular organization and a niche for MSC differentiation *in vivo*.

To understand the biology underlying the repair of critical sized skeletal defects, we and others have developed various bone grafting procedures that include the use of devitalized allografts (donor bone segments derived from a different mouse strain that are processed in a manner to remove all living cells), autografts (live bone grafts that were removed and replaced such that the donor is the same animal as the recipient), and “revitalized” allografts (devitalized allografts that have been treated with cells, growth factors, or any osteoinductive substance that is likely to enhance allograft repair and integration). Characterization of mouse autograft repair demonstrates a coordinated endochondral bone formation process that is initiated from the host and an intramembranous bone formation process that is elicited from the periosteum of the graft at 2-weeks [46]. Allograft repair, on the other hand, is completely dependent upon endochondral bone formation derived from the host at the graft-host cortical junction with no evidence of intramembranous bone formation on the cortical surface of the allografts. This is in part due to the foreign body reaction that

establishes a formal boundary at the host-graft juncture, beyond which cartilage formation and endochondral bone formation cannot occur. By 4 to 6-weeks, autografts appear to have established a mineralized callus that bridges the entire length of the graft. In contrast, bone repair in allografts exhibit markedly less mineralized callus that is typically limited to the host-graft interface region [42]. Our findings presented here demonstrate that MSCs seeded and cultured directly on allografts induces early cartilage formation and enhanced bone formation by 4 weeks post-surgery, but these changes did not lead to a significant increase in biomechanical properties when compared to allograft alone. Moreover, allografts with direct MSC seeding and culturing do not form a bone callus that envelopes the full graft, as is observed in normal autograft repair. This is likely to be the result of MSCs being lost during implantation and throughout the repair process, potentially due to the lack of an appropriate ECM and/or niche. In contrast, data from our MSC sheet groups clearly show a significant increase in new bone that surrounds the length of the graft. Histology further demonstrates that the MSC sheets improve not only early cartilage formation in the callus at 4-weeks, but also subsequent mineralization by 6-weeks resulting in dramatically improved biomechanical properties of the grafted femurs. Interestingly, at 6-weeks post-implantation autografts exhibit biomechanical properties very similar to un-operated, age-matched control femurs [46]. While our MSC sheets induced repair with biomechanical properties (Maximal torque: 20.1±6.9 N.mm and Torsional rigidity: 543.7±148.9 $N.mm^2$/rad) that were dramatically superior to other grafting approaches, these enhanced torsional properties still fall short of age-matched, un-operated femurs (Maximal torque: 24.83±1.98 N.mm and Torsional rigidity: 1332.9.18±81.88 $N.mm^2$/rad)[46]. This indicates that while MSC cell sheet technology is an improved approach to delivering cells for enhancing allograft repair and integration, further research can be done to improve therapeutic efficacy.

## Conclusions

Our data illustrate the remarkable ability of MSC sheets to act as an engineered periosteum that promotes bone callus formation during allograft healing and integration in a mouse femoral defect reconstruction model. These data further suggest that MSC sheets represent a potential clinical treatment to promote osteoblastic bone formation and functional skeletal defect healing in humans. Studies to identify optimal MSC populations for generating cell sheets to achieve repair comparable to autograft healing are currently underway and investigations using large animal models are also being planned to lay the groundwork for future clinical trials.

## Acknowledgments

This work was supported in part by the following grants: NIH/NIAMS R21 grant (AR063803 to YD), Airlift Research Foundation grant (108468 to YD), NIH/NIAMS R01 grants (AR057022 and AR063071 to MJH), R21 grant (AR059733 to MJH), and a NIH/NIAMS P30 Core Center grant (AR061307 to EMS). We also thank Sarah Mack and Kathy Maltby within the Center for Musculoskeletal Research Histology, Biochemistry, and Molecular Imaging Core for their technical expertise.

## References

1. Garbuz DS, Penner MJ. Role and results of segmental allografts for acetabular segmental bone deficiency. Orthop Clin North Am. 1998; 29(2):263–275. [PubMed: 9553572]
2. Stevenson S. Biology of bone grafts. Orthop Clin North Am. 1999; 30(4):543–552. [PubMed: 10471759]
3. Younger EM, Chapman MW. Morbidity at bone graft donor sites. J Orthop Trauma. 1989; 3(3): 192–195. [PubMed: 2809818]
4. Summers BN, Eisenstein SM. Donor site pain from the ilium. A complication of lumbar spine fusion. J Bone Joint Surg Br. 1989; 71(4):677–680. [PubMed: 2768321]

5. Burchardt H, Jones H, Glowczewskie F, Rudner C, Enneking WF. Freeze-dried allogeneic segmental cortical-bone grafts in dogs. J Bone Joint Surg Am. 1978; 60(8):1082–1090. [PubMed: 363723]
6. Chalmers J. Transplantation immunity in bone homografting. J Bone Joint Surg Br. 1959; 41-B(1): 160–179. [PubMed: 13620723]
7. Stevenson S, Shaffer JW, Goldberg VM. The humoral response to vascular and nonvascular allografts of bone. Clin Orthop Relat Res. 1996; (326):86–95. [PubMed: 8620663]
8. Stevenson S, Li XQ, Davy DT, Klein L, Goldberg VM. Critical biological determinants of incorporation of non-vascularized cortical bone grafts. Quantification of a complex process and structure. J Bone Joint Surg Am. 1997; 79(1):1–16. [PubMed: 9010181]
9. Mankin HJ, Gebhardt MC, Jennings LC, Springfield DS, Tomford WW. Long-term results of allograft replacement in the management of bone tumors. Clin Orthop Relat Res. 1996; (324):86–97. [PubMed: 8595781]
10. Lieberman JR, Daluiski A, Einhorn TA. The role of growth factors in the repair of bone. Biology and clinical applications. J Bone Joint Surg Am. 2002; 84-A(6):1032–1044. [PubMed: 12063342]
11. Blokhuis TJ, Lindner T. Allograft and bone morphogenetic proteins: an overview. Injury. 2008; 39 (Suppl 2):S33–36. [PubMed: 18804571]
12. Reynolds DG, Takahata M, Lerner AL, O'Keefe RJ, Schwarz EM, Awad HA. Teriparatide therapy enhances devitalized femoral allograft osseointegration and biomechanics in a murine model. Bone. 2010; 48(3):562–570. [PubMed: 20950720]
13. Smucker JD, Rhee JM, Singh K, Yoon ST, Heller JG. Increased swelling complications associated with off-label usage of rhBMP-2 in the anterior cervical spine. Spine (Phila Pa 1976). 2006; 31(24):2813–2819. [PubMed: 17108835]
14. Shields LB, Raque GH, Glassman SD, Campbell M, Vitaz T, Harpring J, et al. Adverse effects associated with high-dose recombinant human bone morphogenetic protein-2 use in anterior cervical spine fusion. Spine (Phila Pa 1976). 2006; 31(5):542–547. [PubMed: 16508549]
15. Perri B, Cooper M, Lauryssen C, Anand N. Adverse swelling associated with use of rh-BMP-2 in anterior cervical discectomy and fusion: a case study. Spine J. 2007; 7(2):235–239. [PubMed: 17321975]
16. Lieberman JR, Ghivizzani SC, Evans CH. Gene transfer approaches to the healing of bone and cartilage. Mol Ther. 2002; 6(2):141–147. [PubMed: 12161179]
17. Kimelman Bleich N, Kallai I, Lieberman JR, Schwarz EM, Pelled G, Gazit D. Gene therapy approaches to regenerating bone. Adv Drug Deliv Rev. 2012; 64(12):1320–1330. [PubMed: 22429662]
18. Bruder SP, Fink DJ, Caplan AI. Mesenchymal stem cells in bone development, bone repair, and skeletal regeneration therapy. J Cell Biochem. 1994; 56(3):283–294. [PubMed: 7876320]
19. Bruder SP, Jaiswal N, Ricalton NS, Mosca JD, Kraus KH, Kadiyala S. Mesenchymal stem cells in osteobiology and applied bone regeneration. Clin Orthop Relat Res. 1998; (355 Suppl):S247–256. [PubMed: 9917644]
20. Bruder SP, Kraus KH, Goldberg VM, Kadiyala S. The effect of implants loaded with autologous mesenchymal stem cells on the healing of canine segmental bone defects. J Bone Joint Surg Am. 1998; 80(7):985–996. [PubMed: 9698003]
21. Caplan AI, Bruder SP. Mesenchymal stem cells: building blocks for molecular medicine in the 21st century. Trends Mol Med. 2001; 7(6):259–264. [PubMed: 11378515]
22. Kolf CM, Cho E, Tuan RS. Mesenchymal stromal cells. Biology of adult mesenchymal stem cells: regulation of niche, self-renewal and differentiation. Arthritis research & therapy. 2007; 9(1):204. [PubMed: 17316462]
23. Phinney DG, Prockop DJ. Concise review: mesenchymal stem/multipotent stromal cells: the state of transdifferentiation and modes of tissue repair--current views. Stem cells (Dayton, Ohio). 2007; 25(11):2896–2902.
24. Gang EJ, Bosnakovski D, Figueiredo CA, Visser JW, Perlingeiro RC. SSEA-4 identifies mesenchymal stem cells from bone marrow. Blood. 2007; 109(4):1743–1751. [PubMed: 17062733]

25. Sakaguchi Y, Sekiya I, Yagishita K, Muneta T. Comparison of human stem cells derived from various mesenchymal tissues: superiority of synovium as a cell source. Arthritis Rheum. 2005; 52(8):2521–2529. [PubMed: 16052568]
26. Simmons PJ, Torok-Storb B. Identification of stromal cell precursors in human bone marrow by a novel monoclonal antibody, STRO-1. Blood. 1991; 78(1):55–62. [PubMed: 2070060]
27. Digirolamo CM, Stokes D, Colter D, Phinney DG, Class R, Prockop DJ. Propagation and senescence of human marrow stromal cells in culture: a simple colony-forming assay identifies samples with the greatest potential to propagate and differentiate. Br J Haematol. 1999; 107(2): 275–281. [PubMed: 10583212]
28. Tsutsumi S, Shimazu A, Miyazaki K, Pan H, Koike C, Yoshida E, et al. Retention of multilineage differentiation potential of mesenchymal cells during proliferation in response to FGF. Biochemical and biophysical research communications. 2001; 288(2):413–419. [PubMed: 11606058]
29. Zaragosi LE, Ailhaud G, Dani C. Autocrine fibroblast growth factor 2 signaling is critical for self-renewal of human multipotent adipose-derived stem cells. Stem cells (Dayton, Ohio). 2006; 24(11):2412–2419.
30. Go MJ, Takenaka C, Ohgushi H. Forced expression of Sox2 or Nanog in human bone marrow derived mesenchymal stem cells maintains their expansion and differentiation capabilities. Experimental cell research. 2008; 314(5):1147–1154. [PubMed: 18187129]
31. Ming Liu T, Nan Wu Y, Min Guo X, Hoi Po, Hui J, Hin Lee E, Lim B. Effects of Ectopic Nanog and Oct4 Overexpression on Mesenchymal Stem Cells. Stem cells and development. 2008
32. Nishida K, Yamato M, Hayashida Y, Watanabe K, Maeda N, Watanabe H, et al. Functional bioengineered corneal epithelial sheet grafts from corneal stem cells expanded ex vivo on a temperature-responsive cell culture surface. Transplantation. 2004; 77(3):379–385. [PubMed: 14966411]
33. Hasegawa M, Yamato M, Kikuchi A, Okano T, Ishikawa I. Human periodontal ligament cell sheets can regenerate periodontal ligament tissue in an athymic rat model. Tissue Eng. 2005; 11(3–4):469–478. [PubMed: 15869425]
34. Shiroyanagi Y, Yamato M, Yamazaki Y, Toma H, Okano T. Transplantable urothelial cell sheets harvested noninvasively from temperature-responsive culture surfaces by reducing temperature. Tissue Eng. 2003; 9(5):1005–1012. [PubMed: 14633384]
35. Kushida A, Yamato M, Isoi Y, Kikuchi A, Okano T. A noninvasive transfer system for polarized renal tubule epithelial cell sheets using temperature-responsive culture dishes. Eur Cell Mater. 2005; 10:23–30. discussion 23–30. [PubMed: 16088852]
36. Ohki T, Yamato M, Murakami D, Takagi R, Yang J, Namiki H, et al. Treatment of oesophageal ulcerations using endoscopic transplantation of tissue-engineered autologous oral mucosal epithelial cell sheets in a canine model. Gut. 2006; 55(12):1704–1710. [PubMed: 16709659]
37. Shimizu T, Sekine H, Isoi Y, Yamato M, Kikuchi A, Okano T. Long-term survival and growth of pulsatile myocardial tissue grafts engineered by the layering of cardiomyocyte sheets. Tissue Eng. 2006; 12(3):499–507. [PubMed: 16579683]
38. Harimoto M, Yamato M, Hirose M, Takahashi C, Isoi Y, Kikuchi A, et al. Novel approach for achieving double-layered cell sheets co-culture: overlaying endothelial cell sheets onto monolayer hepatocytes utilizing temperature-responsive culture dishes. J Biomed Mater Res. 2002; 62(3): 464–470. [PubMed: 12209933]
39. Takezawa T, Mori Y, Yoshizato K. Cell culture on a thermo-responsive polymer surface. Biotechnology (N Y). 1990; 8(9):854–856. [PubMed: 1366797]
40. Nadri S, Soleimani M, Hosseni RH, Massumi M, Atashi A, Izadpanah R. An efficient method for isolation of murine bone marrow mesenchymal stem cells. Int J Dev Biol. 2007; 51(8):723–729. [PubMed: 17939119]
41. Xie C, Reynolds D, Awad H, Rubery PT, Pelled G, Gazit D, et al. Structural bone allograft combined with genetically engineered mesenchymal stem cells as a novel platform for bone tissue engineering. Tissue Eng. 2007; 13(3):435–445. [PubMed: 17518596]

42. Reynolds DG, Hock C, Shaikh S, Jacobson J, Zhang X, Rubery PT, et al. Microcomputed tomography prediction of biomechanical strength in murine structural bone grafts. J Biomech. 2007; 40(14):3178–3186. [PubMed: 17524409]

43. Thompson RC Jr, Garg A, Clohisy DR, Cheng EY. Fractures in large-segment allografts. Clin Orthop Relat Res. 2000; (370):227–235. [PubMed: 10660718]

44. Zhang X, Awad HA, O'Keefe RJ, Guldberg RE, Schwarz EM. A perspective: engineering periosteum for structural bone graft healing. Clin Orthop Relat Res. 2008; 466(8):1777–1787. [PubMed: 18509709]

45. Mikos AG, McIntire LV, Anderson JM, Babensee JE. Host response to tissue engineered devices. Adv Drug Deliv Rev. 1998; 33(1–2):111–139. [PubMed: 10837656]

46. Yazici C, Takahata M, Reynolds DG, Xie C, Samulski RJ, Samulski J, et al. Self-complementary AAV2. 5-BMP2-coated femoral allografts mediated superior bone healing versus live autografts in mice with equivalent biomechanics to unfractured femur. Mol Ther. 2011; 19(8):1416–1425. [PubMed: 21206485]

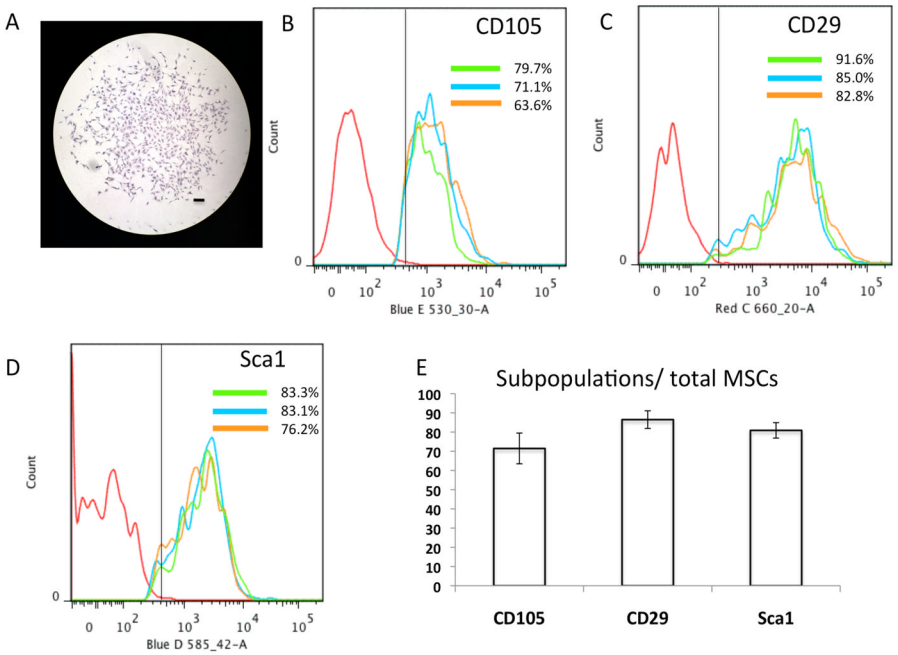


**Figure 1. MSC isolation and characterization**

(**A**) Representative CFU-F colony in the MSC culture visualized by crystal violet staining at day 7. (Scale bars=200μm) (**B**) Representative FACS histograms showing CD105 expression in 3 different isolations of MSCs. (**C**) Representative FACS histograms showing CD29 expression in 3 different isolations of MSCs. (**D**) Representative FACS histograms showing Sca1 expression in 3 different isolations of MSCs. (**E**) Quantification of the CD105, CD29, Sca1 subpopulations in total MSCs. Data are represented as the mean ± SD of three independent experiments performed.

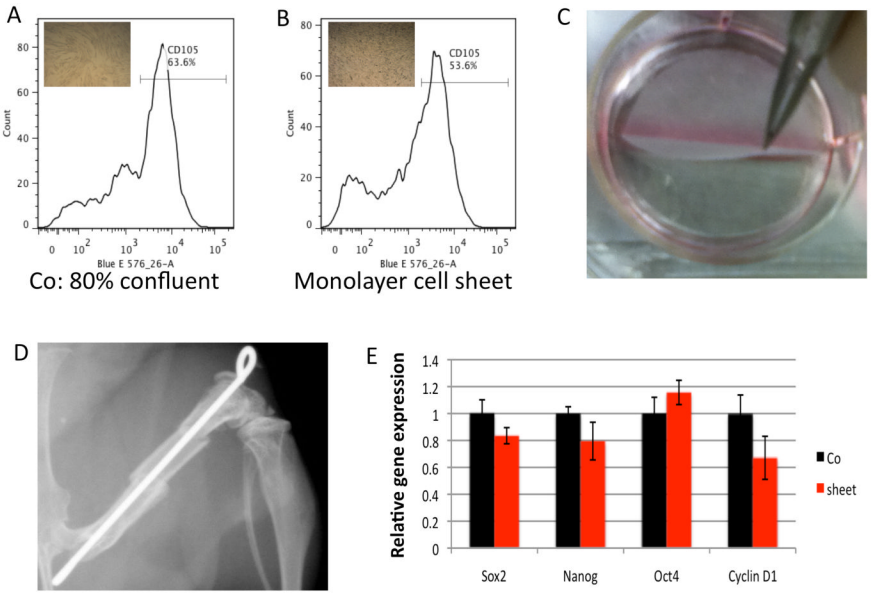


**Figure 2. MSC sheet generation, characterization, and transplantation**

(**A**) Quantification of the CD105 subpopulation in MSCs at 80% confluence. (**B**) Quantification of the CD105 subpopulation in MSCs from cell sheets. (**C**) MSC sheets are easily detached from the dish after 24-hours of culture. (**D**) The x-ray depicts the mouse femoral bone defect and allograft transplantation model used in combination with MSC direct seeding and MSC sheets. (**E**) Comparison of changes in stem cell marker gene expression before (Co) and after formation of the MSC sheet (Sheet). Data are means ± SD of three independent experiments performed in duplicate and the control gene expression level was set at 1.

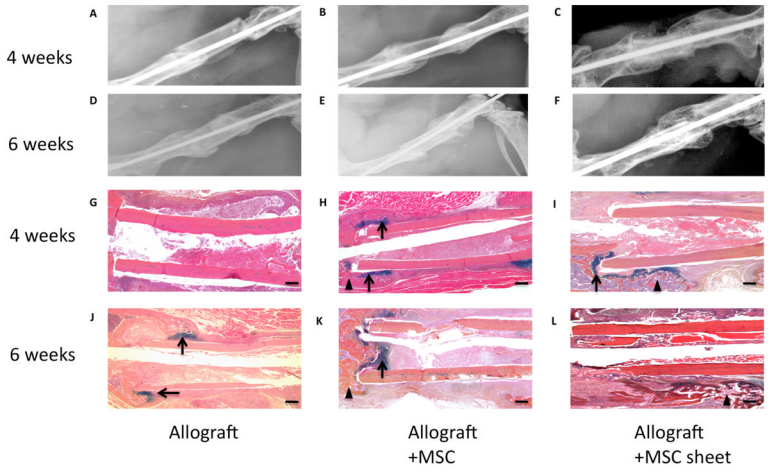


**Figure 3. Effects of MSC seeding and MSC sheets on cartilage and bone formation at 4- and 6-weeks post-surgery**

The upper panels (**A, B, C, D, E, F**) are representative x-ray images of allografts, allografts seeded with MSCs, and allografts wrapped with MSC sheets at 4- and 6-weeks post-surgery. Lower panels (**G, H, I, J, K, L**) show the histological sections stained with AB/H/OG. (Scale bars=400μm). Bone callus is marked with black triangles and cartilaginous callus is marked with black arrows.

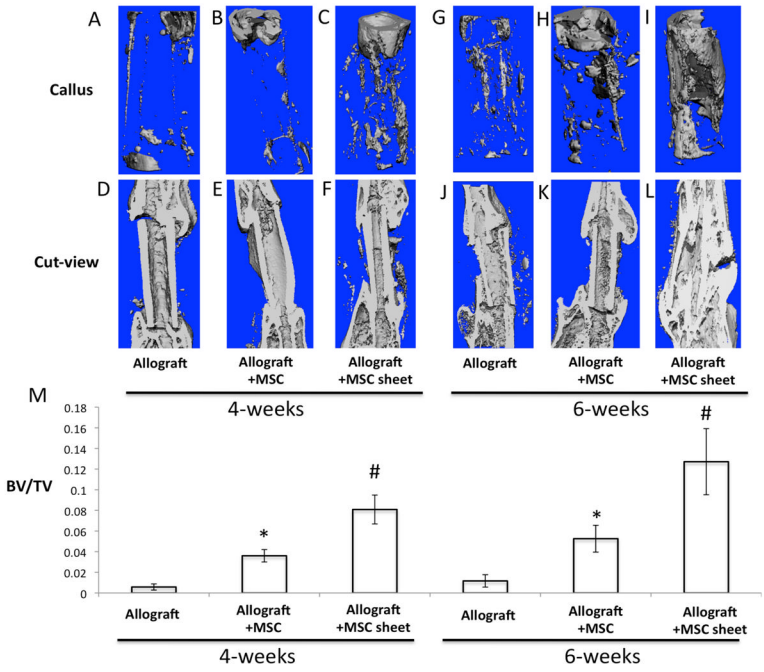


**Figure 4. MSC sheets enhance devitalized allograft osteointegration with host bone, and induces extensive bone callus formation spanning the allograft at 4- and 6-weeks post-surgery**

Representative microCT volumetric rendering of the grafted femurs with direct seeding of MSCs (**B, E, H, K**) and MSC sheets (**C, F, I, L**) at 4- and 6-weeks post-surgery. Allograft alone was used as the control (**A, D, G, J**). Quantification of bone volume/total tissue volume (BV/TV) from the mineralized calluses of each group (M). (*, $p < 0.05$ compared with allograft alone; #, $p<0.05$ compared with allograft + MSC).

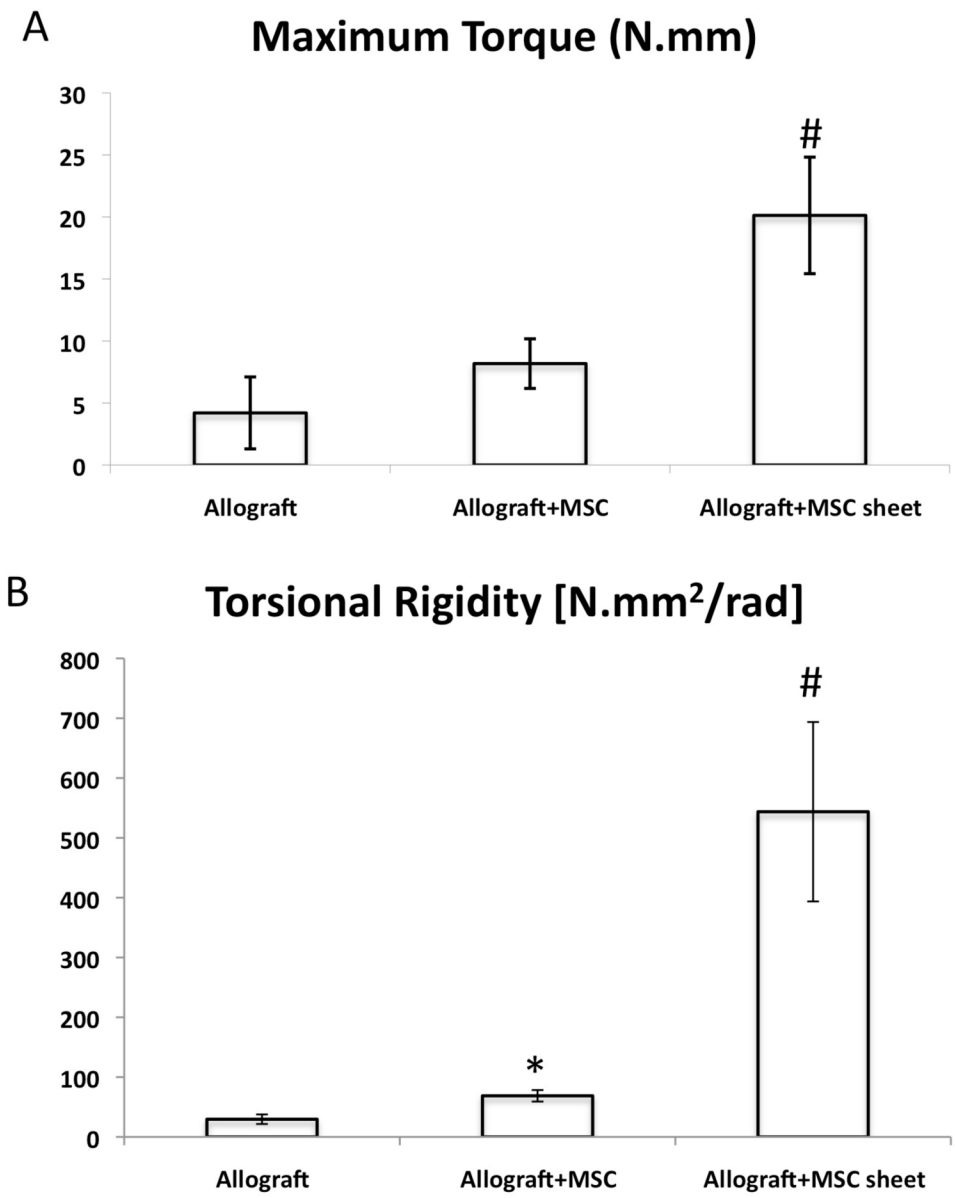


**Figure 5. MSC sheets improve the biomechanical torsional properties of grafted femurs**

Grafted femurs from each group were retrieved upon animal sacrifice at 6-weeks post-surgery and tested in torsion at 1°/sec to determine the maximal torque (**A**) and the torsional rigidity (**B**). Data presented as mean ± standard deviation. (*, $p < 0.05$ compared with allograft alone; #, $p<0.05$ compared with allograft + MSC).

**Table 1**

Mouse primers used for real-time qPCR

| | Forward primer | Reverse primer | Accession number |
|---|---|---|---|
| Sox2 | TACCTCTTCCTCCCACTCCA | CCCTCCCAATTCCCTTGTAT | NM_011443 |
| Oct4 | ACCATGTTTCTGAAGTGCCC | TGGGAAAGGTGTCCCTGTAG | NM_013633 |
| Nanog | CCAAAGGATGAAGTGCAAGC | TTGGTCCAGGTCTGGTTGTT | NM_028016 |
| Cyclin D1 | TGGAGAAGGTACTTACGGTGTGGT | TGGGCACTCCTTCTTCCTCGCT | NM_007659 |
| β-actin | AGATGTGGATCAGCAAGCAG | GCGCAAGTTAGGTTTTGTCA | NM_007393 |